ID-1051

DESIGN OPTIMISATION OF SILO STRUCTURES MADE FROM COMPOSITE MATERIALS

E V Morozov[1], J L Henshall[2] and C J Brown[2]
[1] *School of Mechanical Engineering, University of Natal, Durban, South Africa*
[2] *Department of Mechanical Engineering, Brunel University, Uxbridge, UK*

SUMMARY: This study is concerned with developing a general approach to the problem of optimising the design of cylindrical silos manufactured from composite materials. Minimisation of the material cost was selected as the objective for optimisation. This is considered to be essentially equivalent to minimising the silo's mass. In this paper, the analysis has concentrated upon the cylindrical section of the silo. The design constraints were taken to be: buckling due to axial compression, the maximum stress failure criterion and a defined limiting radial deflection. The analysis also took into consideration the limitations imposed by the chosen manufacturing process, i.e. filament winding. The situation considered was a Class 3 silo subject to loading by a granulate filling material, and was assumed to empty by mass flow. A particular silo geometry and loading have been analysed to illustrate the general methodology. It was found that under normal loading the main design constraint was buckling due to axial compression, with a relatively small region of deflection limited design.

KEYWORDS: Silos; Composite shell structures; Buckling; Design optimisation;

1. INTRODUCTION

The use of the term composite in silo technology more commonly refers to composite structures rather than silos manufactured from fibre reinforced composite materials. However, there are several advantages in using composite materials including good corrosion resistance, lightweight, non-contamination for some contents, and competitive costs. The latter consideration effectively limits the choice of materials to glass fibre reinforced plastics. The preferred manufacturing process for this structural shape is filament winding, which is therefore used in the analysis presented below.

The purpose of the present paper is to demonstrate for this particular application how it is possible to combine the constraints imposed by structural considerations with those of the material, to develop an integrated structural and material design approach [1-2]. This is different from the normal approach of structural design followed by materials selection, even if these two separate aspects are iterated to provide an improved design [1-2]. The current paper demonstrates this approach for the main structural elements of a typical silo, i.e. a cylindrical main holding section with conical hopper. In addition to the usual silo design constraints of buckling and strength [3-5], a constraint arising from the radial deflection of the cylindrical part of silo is also imposed, since it is known that the low stiffness of structures composed of fibre composites may cause problems in service. The design of the vertical cylindrical section is considered in the paper. A typical silo geometry is used as an example of the application of the general approach.

2. SILO GEOMETRY, LOADING AND DESIGN SITUATIONS.

For slender silos, the filling loads when it is symmetrically filled are the wall frictional pressure p_{wf}, horizontal pressure p_{hf} and vertical pressure p_v. According to [3], the values of these loads at any depth z (see Fig. 1) are taken as:

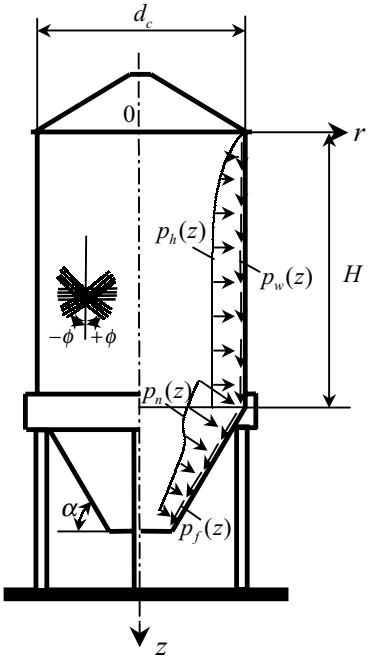

Fig.1 Silo geometry and loading

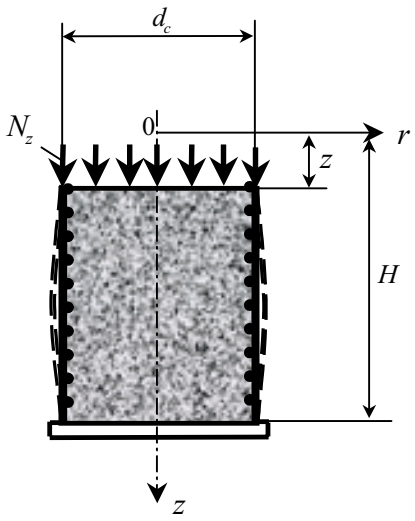

Fig. 2 Schematic diagram of buckling model for appropriate portion of vertical cylindrical part of silo

$$p_{wf}(z) = \gamma \frac{A}{U} C_z(z) \tag{2.1}$$

$$p_{hf}(z) = \frac{\gamma A}{\mu U} C_z(z) \tag{2.2}$$

$$p_v(z) = \frac{\gamma A}{K_s \mu U} C_z(z) \tag{2.3}$$

C_z is the Janssen coefficient, i.e.

$$C_z(z) = 1 - e^{(-z/z_0)}, \qquad z_0 = \frac{A}{K_s \mu U}$$

where γ is the weight density of the filling material, μ is the wall friction coefficient, K_s is the horizontal/vertical pressure ratio, U is the internal perimeter, and A is the cross-sectional area of vertical walled section. For a cylindrical silo, the parameter z_0 is given by:

$$z_0 = \frac{d_c}{4K_s \mu}$$

where d_c is the diameter of cylindrical part of the structure (see Fig. 1). Correspondingly, the pressure components (2.1) – (2.3) now become:

$$p_{wf}(z) = \gamma \frac{d_c}{4}(1 - e^{-z/z_0}) \tag{2.4}$$

$$p_{hf}(z) = \frac{\gamma}{\mu} \cdot \frac{d_c}{4}(1 - e^{-z/z_0}) \tag{2.5}$$

$$p_v(z) = \frac{\gamma}{K_s \mu} \cdot \frac{d_c}{4}(1 - e^{-z/z_0}) = \gamma z_0 (1 - e^{-z/z_0}) \tag{2.6}$$

The resulting vertical force in the wall, $P_w(z)$ per unit length of perimeter, acting at any depth z is

$$P_w(z) = \int_0^z p_{wf}(z) dz$$

which, combined with (2.4) gives:

$$P_w(z) = \gamma \frac{d_c}{4} \left[z - z_0 (1 - e^{-z/z_0}) \right] \tag{2.7}$$

The discharge loads for the vertical walled section of the structure, p_{we} and p_{he}, are calculated as follows

$$p_{we} = C_w p_{wf} \qquad\qquad p_{he} = C_h p_{hf}$$

where C_w and C_h are load magnifiers which for slender silos are [3]:

$$C_w = 1.1 \qquad\qquad C_h = C_0 \tag{2.8}$$

where the value of coefficient C_0 depends on the type of particulate material and can be found in [3]. The coefficients presented by (2.8) are accounting for the increase in loading during discharge. In the present analysis these coefficients are combined into an effective overall safety factor. The analysis is restricted to consideration of buckling under axial compression and bursting or rupture under internal pressure according to the design cases presented in [4]. This corresponds to the actions of filling, storage and discharge of particulate solids. The design is based on the ultimate limit states and the possible unsymmetrical loading is accounted for by the increased values of the respective safety factors. The results of the design optimisation in this work are directly applicable to the silos in Reliability Class 3 [4] and silos with $d_c < 5\,\mathrm{m}$ [3]. In the case of the design situations and action combinations for Reliability Classes 1 and 2 (including unsymmetrical loading, free patch loads, etc.), additional analyses should be performed to refine the values of the structural parameters. There are some specific loading cases that may need to be considered at the design stage, depending on the type of filling material. Dust explosions may occur with some granulate materials stored in the silos. Correspondingly, the loads due to dust explosions are classified in DD ENV 1991-4 [3] as an accidental action. The potential damage from dust explosions should be limited or avoided by appropriate choice of one or both of the following: incorporating sufficient pressure relief area and/or designing the structure to resist the explosion pressure. The explosion pressure in a silo without adequate relief area may be as high as $1\,\mathrm{N/mm^2}$. The loads on the hopper are determined by the pressure normal to the inclined hopper wall p_n and the wall frictional pressure p_t as shown in Fig. 1.

3.DESIGN OPTIMISATION OF THE VERTICAL CYLINDRICAL SECTION OF THE SILO

Taking into account the requirements for the silo structure to withstand a variety of axisymmetric (internal pressure, friction forces) and possible unsymmetrical loading (wind load, patch loads, etc.), it was decided that the composite layer's distribution across the wall

thickness should be symmetrical. This would provide the highest level of bending stiffness for the composite wall [6]. The analysis is also restricted to three layers in total for practical considerations with this relatively thin-walled structure. The laminate wall structure is assumed to be [90°/±ϕ/90°]. The introduction of 90^{o} - oriented layers is based on the simplicity and cost efficiency of the implementation of circumferential filament winding for composite silo production. It is also appropriate to have this type of reinforcement to withstand any applied internal pressure. The helical angle ϕ of the reinforcement orientation (see Fig. 1) is determined by the design optimisation procedure. The other two unknown design parameters, for given geometry and dimensions of a silo, are the thicknesses of the layers, i.e. h_{90} and h_{ϕ}.

As was discussed in Section 2, the design of the cylindrical wall of the silo is performed in this work by considering buckling under axial compression and bursting or rupture under internal pressure. An additional constraint arising from the deflection of the cylindrical part of the silo is also imposed, since it is known that the relatively low stiffness of structures composed of glass fibre composites may cause problems in service.

3.1 Buckling due to Axial Compression

As was discussed in Section 2 the cylindrical portion of the silo is loaded along its length by the frictional forces resulting in axial compression. The resulting vertical force in the wall $P_w(z)$ per unit length of perimeter acting at any depth z is calculated according to equation (2.7). The critical compressive load per unit circumference N_z^{cr} for a cylinder of length L can be found from the following equation [7]:

$$\frac{N_z L^2}{\pi^2 D_{11}} = m^2\left(1+2\frac{D_{12}}{D_{11}}\xi^2+\frac{D_{22}}{D_{11}}\xi^4\right)+\frac{\tilde{\gamma}L^4}{\pi^4 m^2 D_{11}(d_c/2)^2}\cdot\frac{B}{B_{11}+\left(\frac{B}{B_{44}}-2B_{12}\right)\xi^2+B_{22}\xi^4} \tag{3.1}$$

where $\xi=\frac{2nL}{\pi d_c m}$, $\tilde{\gamma}=1-0.901(1-e^{-\psi})$, and $\psi=\frac{1}{29.8}\left(\frac{d_c}{2}\right)^{1/2}\left(\frac{D_{11}D_{22}}{B_{11}B_{22}}\right)^{-1/8}$.

Here, m is the number of buckle half waves in the axial direction, n is the number of buckle waves in the circumferential direction, and $\tilde{\gamma}$ is an empirical (knock down) factor that insures that the calculated buckling load will be conservative with respect to all available experimental data [8]. The stiffness coefficients are calculated as follows:

$$B_{kl}=\int_{-h/2}^{h/2}A_{kl}dy,\quad D_{kl}=\int_{-h/2}^{h/2}A_{kl}y^2dy,\ (k,l=1,2),\ B=B_{11}B_{22}-B_{12}^2$$

where the parameters A_{kl} are defined in [6] in terms of the mechanical properties of the elementary composite layers and angles of the reinforcement orientation. Equation (3.1) is valid for the mid-plane symmetry of the shell wall. The current design situation is quite specific due to the particular form of the load application. The shell is filled in with a granulate. This means that the wall is supported from the inside by the filling material. However, the nature of the supporting internal pressure is different from the situation when the shell is filled with gas or liquid. The conditions at the internal surface throughout the shell are close to the sliding/rolling continuous unilateral simple support as shown in Fig. 2. This support prevents the shell from deflections directed towards the axis of the shell (into the

shell), but leaves freedom for the wall to be bent out along the meridian under compressive axial loading. The magnitude of the compressive load is determined by the friction forces and calculated according to equation (2.7) for a given depth z. According to this model (see Fig.2), it is possible to restrict the consideration of the initial buckling in the small deflection range to one possible mode known as symmetrical or 'ring' buckling. Taking $n = 0$, and $m = 1$ equation (3.1) reduces to the form:

$$N_z = D_{11}\left[\frac{\pi^2}{L^2} + \tilde{\gamma}^2 \frac{4L^2}{\pi^2 D_{11} d_c^2} \cdot \frac{B}{B_{11}}\right] \tag{3.2}$$

where $L = H - z$ is the part of the shell loaded with the resulting vertical force in the wall $P_w(z)$ (see equation (2.7)). To find the minimum buckling load, N_z^{cr}, the derivative of N_z with respect to L is set equal to zero. The length at which the minimum buckling load occurs is

$$L_{cr} = \pi\left[\frac{D_{11} d_c^2}{4\tilde{\gamma}^2} \cdot \frac{B_{11}}{B}\right]^{1/4} = H - z^* \tag{3.3}$$

where z^* is the corresponding critical depth of the silo, and the minimum buckling load is

$$N_z^{cr} = \frac{4D_{11}\tilde{\gamma}}{d_c}\left(\frac{D_{11}B_{11}}{B}\right)^{-1/2} \tag{3.4}$$

According to this, the silo design should be performed subject to the following constraint:

$$P_w(z^*) \le N_z^{cr} \tag{3.5}$$

Substituting for $P_w(z)$ and N_z^{cr} from equations (2.7) and (3.4), and taking into account equation (3.3), gives:

$$\gamma \frac{d_c}{4}\left[z^* - z_0\left(1 - e^{-\frac{z^*}{z_0}}\right)\right] \le \frac{4D_{11}\tilde{\gamma}}{d_c}\left(\frac{D_{11}B_{11}}{B}\right)^{-1/2} \tag{3.6}$$

where $z^* = H - \pi\left(\frac{D_{11} d_c^2}{4\tilde{\gamma}^2} \cdot \frac{B_{11}}{B}\right)^{1/4}$.

For the case under consideration, the stiffness coefficients B_{kl} and D_{kl} $(k,l = 1,2)$ are calculated as follows:

$$\begin{aligned} B_{kl} &= h_\phi A_{kl}^{(1)} + h_{90} A_{kl}^{(2)} \\ D_{kl} &= \frac{2}{3}\left\{A_{kl}^{(1)}\left(\frac{h_\phi}{2}\right)^3 + A_{kl}^{(2)}\left[\left(\frac{h_\phi + h_{90}}{2}\right)^3 - \left(\frac{h_\phi}{2}\right)^3\right]\right\} \end{aligned} \tag{3.7}$$

where h_ϕ is the thickness of helical layer oriented at an angle $\phi_1 = \phi$ to the cylinder generatrix, and h_{90} is the total thickness of the circumferential layers ($\phi_2 = 90^\circ$). The coefficients $A_{kl}^{(i)}$ $(i = 1,2)$ are determined by the following relationships [6]

$$A_{11}^{(i)} = \overline{E}_1 \cos^4 \phi_i + \overline{E}_2 \sin^4 \phi_i + 2(\overline{E}_1 \nu_{12} + 2G_{12}) \sin^2 \phi_i \cos^2 \phi_i$$

$$A_{22}^{(i)} = \overline{E}_1 \sin^4 \phi_i + \overline{E}_2 \cos^4 \phi_i + 2(\overline{E}_1 \nu_{12} + 2G_{12}) \sin^2 \phi_i \cos^2 \phi_i \tag{3.8}$$

$$A_{12}^{(i)} = \overline{E}_1 \nu_{12} + (\overline{E}_1 + \overline{E}_2 - 2(\overline{E}_1 \nu_{12} + 2G_{12})) \sin^2 \phi_i \cos^2 \phi_i \quad (i = 1,2)$$

where, $\overline{E}_{1,2} = E_{1,2} / (1 - \nu_{12} \nu_{21})$. Equations (3.8) include effective or apparent longitudinal, E_1, transverse, E_2, and shear, G_{12}, moduli of a ply and Poisson's ratios ν_{12} and ν_{21} ($E_1 \nu_{12} = E_2 \nu_{21}$).

3.2 Strength Analysis

Under internal pressure and friction load, the necessary level of design resistance should be provided at every point in the shell. Given the load distribution shown in Fig. 1, the cross section with the highest stresses is situated at the bottom of the cylinder ($z = H$). Using equations (2.4) and (2.5), the membrane stress resultants acting in this cross section are calculated as follows:

$$N_z = -\gamma_s \cdot \gamma \frac{d_c}{4} [H - z_0 (1 - e^{-H/z_0})] \qquad N_\theta = \gamma_s \frac{\gamma}{\mu} \cdot \frac{d_c^2}{8} (1 - e^{-H/z_0}) \tag{3.9}$$

where γ_s is the safety factor.
The meridional and circumferential strains are determined by the following equations:

$$\varepsilon_z = (N_z B_{22} - N_\theta B_{12}) / B \qquad \varepsilon_\theta = (N_\theta B_{11} - N_z B_{12}) / B \tag{3.10}$$

The stresses acting in the elementary layers of the composite should not exceed the corresponding limit values. For design purposes, the maximum stress failure criterion was implemented. According to this condition the following set of relationships should be satisfied for each *i*-th elementary layer:

$$\sigma_1^{(i)} \le \overline{\sigma}_1^+ \quad \sigma_2^{(i)} \le \overline{\sigma}_2^+ \quad \text{if } \sigma_1^{(i)} > 0 \quad \sigma_2^{(i)} > 0$$

$$\left|\sigma_1^{(i)}\right| \le \overline{\sigma}_1^- \quad \left|\sigma_2^{(i)}\right| \le \overline{\sigma}_2^- \quad \text{if } \sigma_1^{(i)} < 0 \quad \sigma_2^{(i)} < 0 \tag{3.11}$$

$$\left|\tau_{12}^{(i)}\right| \le \overline{\tau}_{12}$$

For a plane stress state of an orthotropic layer, this approach requires at least five experimental results specifying material strength under longitudinal tension, $\overline{\sigma}_1^+$, longitudinal compression, $\overline{\sigma}_1^-$, transverse tension, $\overline{\sigma}_2^+$, transverse compression, $\overline{\sigma}_2^-$, and in-plane shear, $\overline{\tau}_{12}$.
The corresponding stresses are calculated as follows:

$$\sigma_1^{(i)} = \overline{E}_1 (\varepsilon_1^{(i)} + \nu_{12} \varepsilon_2^{(i)}) \qquad \sigma_2^{(i)} = \overline{E}_2 (\varepsilon_2^{(i)} + \nu_{21} \varepsilon_1^{(i)}) \qquad \tau_{12}^{(i)} = G_{12} \gamma_{12}^{(i)} \tag{3.12}$$

Here, the strains of the *i*-th elementary layer are determined in terms of the meridional ε_z and circumferential ε_θ strains and angle of reinforcement orientation ϕ_i

$$\varepsilon_1^{(i)} = \varepsilon_z \cos^2 \phi_i + \varepsilon_\theta \sin^2 \phi_i \quad \varepsilon_2^{(i)} = \varepsilon_z \sin^2 \phi_i + \varepsilon_\theta \cos^2 \phi_i \quad \varepsilon_{12}^{(i)} = (\varepsilon_\theta - \varepsilon_z) \sin 2\phi_i \tag{3.13}$$

where the strains ε_z and ε_θ are calculated according to equations (3.10).

The set of inequalities (3.11), (including equations (3.7)-(3.10) and (3.12), (3.13)) represents a formalisation of the strength constraints imposed on the design parameters: ϕ, h_ϕ and h_{90}.

3.3 Radial Deflection Constraint

To prevent excessive radial deformations of the shell and provide the necessary stiffness of the structure made from polymer composite materials the design should be performed subject to the following constraint

$$w \le \overline{w} \tag{3.14}$$

where the radial deflection of the shell *w* is calculated as follows

$$w = \frac{d_c}{2B}(N_\theta B_{11} - N_z B_{12}) \tag{3.15}$$

and $\overline{w}$ is the limit value of this parameter, with the stress resultants as determined by equations (3.9).

3.4 Formulation of the Design Optimisation Problem

Minimisation of the material cost as a part of the cost effective silo design was considered as the objective for optimisation in this case. Correspondingly the minimum mass of the silo structure was selected as the objective function. In terms of the design variables introduced earlier for the problem under consideration, the minimum value of the objective function will be delivered if the following condition is satisfied

$$h = h_{90} + h_\phi \quad \rightarrow \quad \textbf{min} \tag{3.16}$$

subject to the set of constraints (see Sections 3.1-3.3):

- buckling of the cylindrical section

$$\gamma_s \cdot \gamma \frac{d_c}{4}\left[z^* - z_0(1 - e^{-z^*/z_0})\right] \le \frac{2\tilde{\gamma}}{R} \cdot \left(\frac{D_{11}B}{B_{11}}\right)^{1/2} \tag{3.17}$$

- limited radial deflection

$$w = \frac{R}{B}(N_\theta B_{11} - N_z B_{12}) \le \overline{w} \tag{3.18}$$

- strength conditions

$$\begin{gathered} \sigma_1^{(i)} \le \overline{\sigma}_1^{+} \text{ for } \sigma_1^{(i)} > 0, \quad \left|\sigma_1^{(i)}\right| \le \overline{\sigma}_1^{-} \text{ for } \sigma_1^{(i)} < 0 \\ \sigma_2^{(i)} \le \overline{\sigma}_2^{+} \text{ for } \sigma_2^{(i)} > 0, \quad \left|\sigma_2^{(i)}\right| \le \overline{\sigma}_2^{-} \text{ for } \sigma_2^{(i)} < 0 \\ \tau_{12}^{(i)} \le \overline{\tau}_{12} \end{gathered} \tag{3.19}$$

where γ_s is the safety factor. The optimum values of the design parameters $\hat{\phi}$, $\hat{h}_\phi$ and $\hat{h}_{90}$ deliver the minimum value of the objective function (3.16) subject to the conditions presented by relationships (3.17)-(3.19).

4. EXAMPLE

The relevant geometric and material property data for the particular design example considered in this study are:
Silo geometry: $H = 7000$ mm, $d_c = 2600$ mm and $\alpha = 60°$.
Particulate material (barley) properties: weight density $\gamma = 8.5$ kN/m^3, $K_s = 0.55$, $\mu = 0.4$, and $\gamma_s = \gamma_f \gamma_m = 1.7$, $\gamma_h = \gamma_{M1}\gamma_F = 1.7$ [3].
Composite material (glass-epoxy) properties: $\delta = 0.6\,\text{mm}$, $E_1 = 44$ GPa, $E_2 = 9.4$ GPa, $G_{12} = 4$ GPa, $\nu_{21} = 0.26$, $\bar{\sigma}_1^+ = 1470\,\text{MPa}$, $\bar{\sigma}_1^- = 650\,\text{MPa}$, $\bar{\sigma}_2^+ = 40\,\text{MPa}$, $\bar{\sigma}_2^- = 90\,\text{MPa}$, $\bar{\tau}_{12} = 50\,\text{MPa}$ and $\bar{w} = 1\,\text{mm}$.

To solve the design problem presented by Eqs. (3.16)-(3.19) the inequalities (3.17)-(3.19) were converted into equalities which determine the boundaries of the feasible domains for the design variables ϕ, h_ϕ and h_{90} in the corresponding 3D design space. As a result of the numerical solutions of the equations obtained with such conversion, the combined feasible domain for the design parameters was constructed. The resultant limiting 3D-surface reflecting the buckling and deflection constraints is shown in Fig. 3. It was found that for the

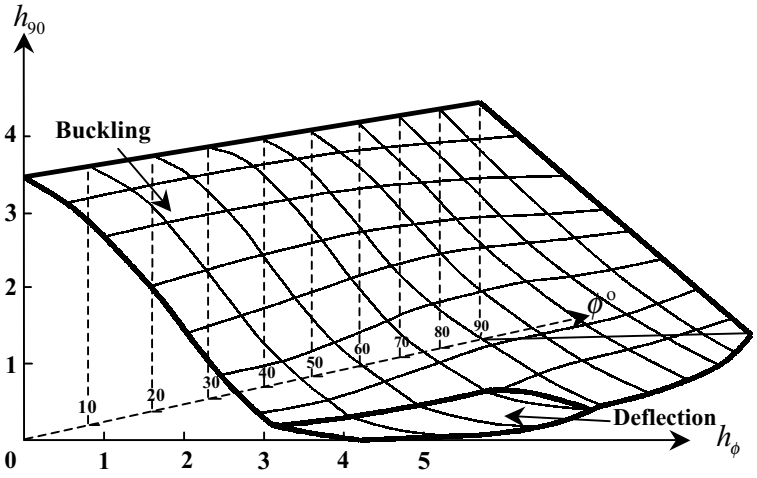

Fig. 3 Boundary surface for buckling constraint

major part of the feasible design space buckling was the active constraint. For a small region, with $\phi \le 30^o$ and $h_{90} \le 0.3\,\text{mm}$, deflection becomes the active constraint. For the considered case and data specification, the strength constraints (3.19) do not play a significant role and are inactive. Due to the specific analytical form of the objective function (3.16), it is possible to locate the optimum values for the design parameters h_ϕ and h_{90} for every value of the reinforcement angle ϕ. The lines of constant values h_{const} of the objective function (3.16) are determined by the equation

$$h_{90} = h_{\text{const}} - h_\phi \tag{4.1}$$

for each value of angle ϕ. Geometrically, this equation represents a family of planes oriented at angles of 45^o to the coordinate planes (h_ϕ, ϕ) and (h_{90}, ϕ) in the 3D- case for different values of h_{const}, or the corresponding families of lines oriented at angles of 45^o to the axes h_ϕ and h_{90} of the two-dimensional coordinate frames for given values of angle ϕ. This allows the optimum values of the design parameters within the given feasible domains to be found.

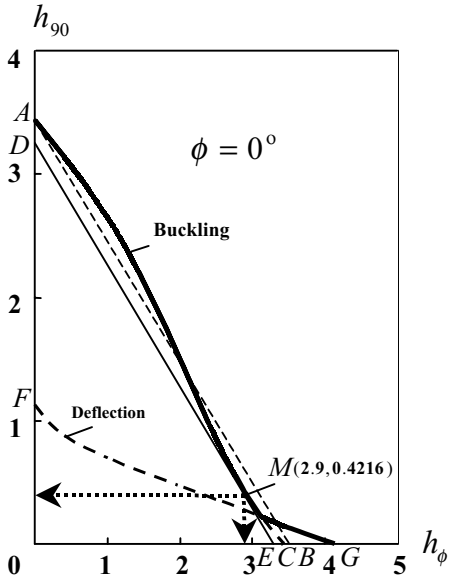

Fig. 4 Feasible domain for $\phi = 0^{\circ}$, (———) - the joint boundary of the feasible domain; (– – – –) - the deflection constraint boundary; (——— , ----------) - the objective function constant value lines

Graphical interpretation of the solution is illustrated in Figures (4)-(6) where all the aforementioned components (objective function constant value lines and constraints) are plotted for $\phi = 0^{\circ}$ (Fig. (4)), $\phi = 30^{\circ}$ (Fig. (5)), and $\phi = 60^{\circ}$ (Fig. (6)). As can be seen, Fig. 4, the optimum point *M* has the coordinates $\hat{\phi} = 0^{\circ}$, $\hat{h}_{\phi} = 2.9\,\text{mm}$ and $\hat{h}_{90} = 0.4216\,\text{mm}$. This point is the point of tangency of the line *DE* determined by the equation (4.1) and curve *AC* that represents the buckling constraint according to equation (3.17). The boundary of the feasible domain is presented by the combination of the buckling and deflection (curve *FG*) constraints.

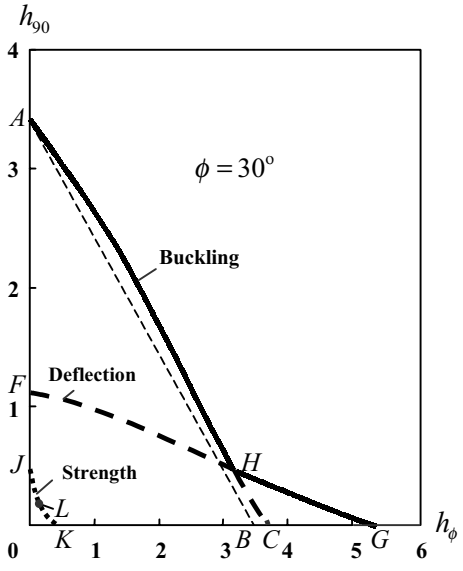

Fig. 5 Feasible domain for $\phi = 30^{\circ}$

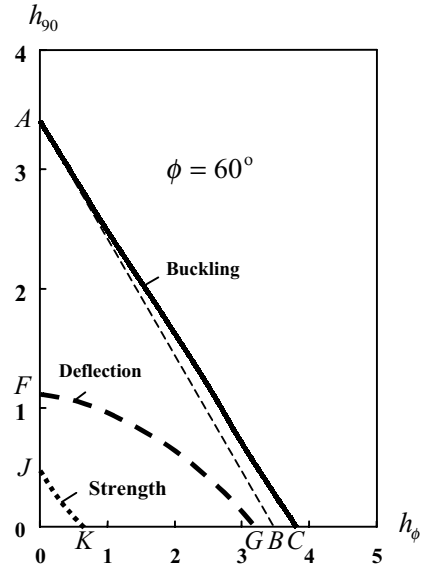

Fig. 6 Feasible domain for $\phi = 60^{\circ}$

The level of stresses caused by the specified load for this example is low. To illustrate this fact the limit curves *JK* (boundaries) are shown in Fig.5 and Fig.6 by dotted lines. For $\phi = 30^{\circ}$ the limit curve consists of two parts *JL* and *LK*. The first part is determined by the

condition $\sigma_2^{(2)} = \overline{\sigma}_2^+$, and the second one by the equation $\tau_{12}^{(1)} = \overline{\tau}_{12}$. In these equations, the superscripts 1 and 2 correspond to the layer reinforcement angles ϕ of 30° and 90° respectively. For $\phi = 60^o$, the limit curve *JK* is determined by the equation $\sigma_2^{(2)} = \overline{\sigma}_2^+$ only. In both cases the values of design parameters are determined by the transverse strength characteristics of the composite materials that are quite low, especially in comparison with the strength of the material along the fibres. Nevertheless, as was mentioned above, the strength constraints did not affect the solution of the problem, which was controlled mainly by the buckling condition with the deflection constraint for a relatively small part of the design space. In all cases, the thicknesses required to meet the stress limiting constraints are much less than those determined by the buckling and deflection (see Figures 5-6). According to the character of the limiting surface determined by the buckling constraint (see Figures 3-6) for angles $\phi \geq 15^o$ the optimum design parameters would be equal to $\hat{\phi} = \phi$, $\hat{h}_\phi = 0$ and $\hat{h}_{90} = 3.44\,\text{mm}$ (see Figures 5-6) providing the same constant value of the objective function $h = h_\phi + h_{90} = 3.44\,\text{mm}$. The minimum thickness corresponding to point *M* (see Fig. 4) occurs for *h* = 3.32 mm. The greatest value of total thickness lying on the design surface is *h* = 3.84 mm, which is 16% higher than the minimum thickness.

5. CONCLUSIONS

The paper describes an approach to the problem of design optimisation of silo structures made from composite materials. The design of the vertical cylindrical section fabricated by the filament winding is considered. The analysis is restricted to consideration of buckling under axial compression and bursting or rupture under internal pressure of the silo loaded by the granulate filling material, which was assumed to empty by mass flow. It was found that the strength constraints did not affect the solution of the problem, which was controlled mainly by the buckling condition with deflection constraint for some part of the design space. In all cases the thicknesses required to meet the stress limiting constraints are much less than those determined by buckling and deflection. The results of the design optimisation in this work are directly applicable to the silos in Reliability Class 3 [4] and silos with $d_c < 5\,\text{m}$ [3].

REFERENCES

1. Morozov, E.V. Chapter 8. “Optimum design of filament wound composite shells”, Optimal Structural Design. Edited by V.V. Vasiliev and Z. Gurdal. Technomic Publ.Co., Inc., Lancaster, PA 17604, 1998.
2. Morozov, E.V. “Structural optimization of multilayered and multizonal composite shells”, *Proceeding of the International Conference “Mechanics in Design”(MID’98),* Nottingham, UK, 6-9 July 1998, Chandos Publ. (Oxford) Ltd., 1998, pp. 356 - 364.
3. DD ENV 1991-4: 1996 Eurocode 1: “Basis of design and actions on structures”, Part 4: Actions in silos and tanks.
4. D prENV 1993-4-1: 1997 Eurocode 3: “Design of steel structures”, Part 4-1: Silos.
5. Rotter, J.M. “Structural design of silos and the new Eurocodes”, *ImechE Conference Transactions* 2000-3, (2000), pp. 153-167.
6. Vasiliev, V.V. and Morozov, E.V. Mechanics and Analysis of Composite Materials, Elsevier Science, 2001.
7. Vinson, J.R. and Sierakowski, R.L. The Behavior of Structures Composed of Composite Materials, Martinus Nijhoff Publishers, 1986.
8. Weingarten, V.I., Seide, P., and Peterson, J.P. Buckling of thin-walled circular cylinders. NASA SP-8007, 1968.